**Natural Hazards
and Earth
System Sciences**

Comparing historical-hydrogeomorphological reconstitution and hydrological-hydraulic modelling in the estimation of flood-prone areas – a case study in Central Portugal

P. P. Santos[1]**, A. O. Tavares**[2]**, and A. I. A. S. S. Andrade**[3]

[1]Centre for Social Studies, University of Coimbra, Portugal
[2]Centre for Social Studies and Department of Earth Sciences, University of Coimbra, Portugal
[3]Centre for Geophysics, Department of Earth Sciences, University of Coimbra, Portugal

Abstract. The Arunca River basin in Central Portugal has a historical record of hazardous events related to floods, causing widespread disturbance. This article describes the application of two approaches based on well-known methods for the estimation of flood-prone areas: (i) historical-hydrogeomorphological reconstitution, applied to the entire Arunca River basin, and (ii) hydrological-hydraulic modelling, applied to four sections selected from different (upper, middle and lower) sectors of the basin and including urban and rural areas along the Arunca River. The mapping of the flood-prone areas obtained by these two methods was compared in order to identify the main differences and similarities. Human interventions (river channel and floodplain morphological changes) were found to be the main factor explaining the differences and similarities between the results obtained by both methods. The application of hydrological-hydraulic modelling proved important in reinforcing the results of the historical-hydrogeomorphological method; it also helped in complementing the results produced by the latter method in urban areas and in areas with insufficient historical records. The application of the historical-hydrogeomorphological method, in turn, allowed for the size of the flood-prone areas to be determined where the primary data (e.g. geometry, roughness and flow) was not accurate enough for hydrological-hydraulic modelling. The methodological approach adopted demonstrates the strong complementary relationship between the different existing methods for estimating flood-prone areas, and may be reproduced for other drainage basins.

1 Introduction

River floods, associated with social and economic damage and loss (UNISDR, 2009), are a major concern in many regions of the world and have been featured in a statement on scientific strategies and public policy management (USGS, 2007; IFRCRCS, 2009). In Europe, these hazardous processes have become one of the topics in land use planning, public policies for risk prevention and reduction, and early warning and emergency measures and resources (Coeur and Lang, 2008; Kubal et al., 2009; Merz et al., 2010).

The evaluation of flood-prone areas using a comprehensive modelling approach commonly targets the performance of different methods and models, with implications for spatial display (Casas et al., 2006; Fewtrell et al., 2008; de Moel et al., 2009). Frequently, the lack of available data sets and accurate flow geometry and dynamics presents new challenges for the design and calibration of hydraulic flood models. Several attempts have focused on transferring hydrological outputs to hydraulic models (Benito et al., 2003; Neal et al., 2009; Gül et al., 2010).

The use of historical data for past floods has been cited in different studies as an improvement on the uncertainty of extreme events (Barriendos et al., 2003; Coeur and Lang, 2008; Sudhaus et al., 2008) and hydrogeomorphological reconstitution has made descriptions of anthropogenic flood control possible (Spaliviero, 2003; Forte et al., 2005; Nirupama and Simonovic, 2007). These approaches and resources have also been used to support hydrological and hydraulic calculations (e.g. Ballais et al., 2005; Vijay et al., 2007; Apel et al., 2009; Neal et al., 2009).
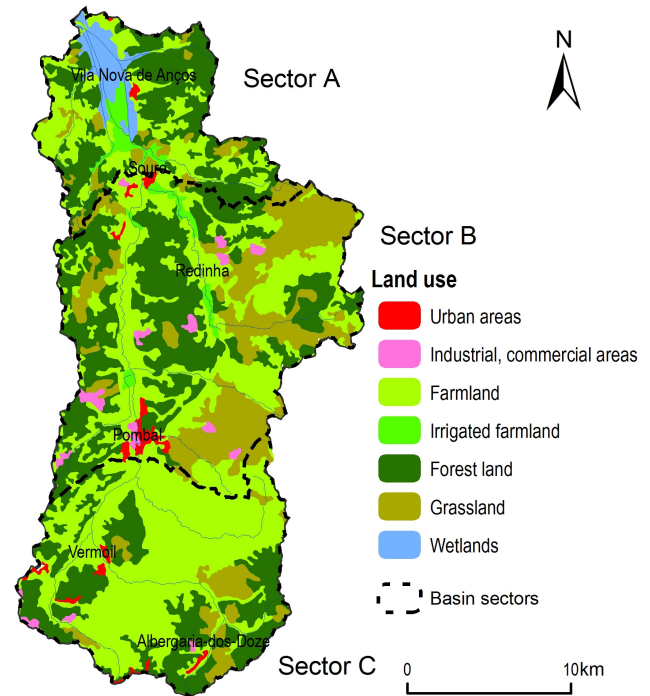
The need to make use of historical data and/or hydrogeomorphological reconstitutions of past flood events to support the modelling of hydraulic flow is often the result of
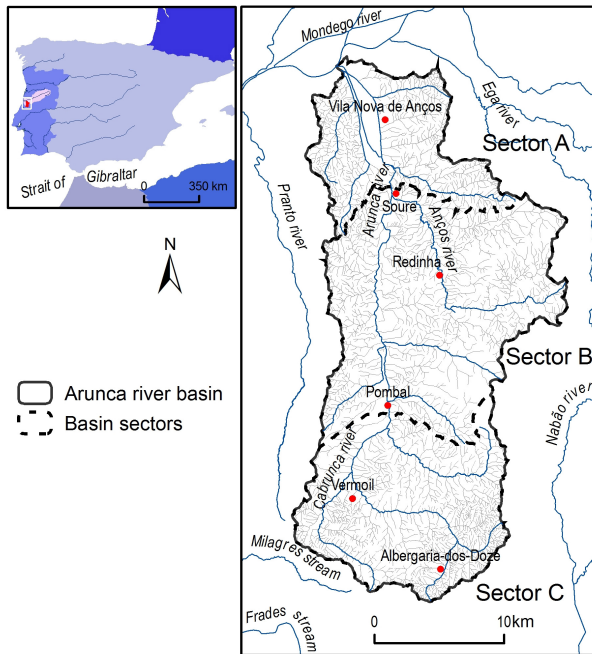
Fig. 1. Location of the Arunca River drainage basin (Central Portugal) and basin sectors.

Fig. 2. Arunca River basin land use.

insufficient information for model calibration, due to a lack of peak discharge, channel geometry and roughness data.

This paper deals with two different methodological approaches to flood dimensions – the historical reconstitution of past events associated with hydrogeomorphological conditions, and hydrological-hydraulic modelling. This integrated analysis has made flood risk assessment possible with reinforced data and quality control for cartographic output. Cross checking was carried out, focussing on a reliable definition of flood impacts in a local context, which has been the goal of different authors and case studies (Nirupama and Simonovic, 2007; Barroca et al., 2006; Spaliviero, 2003; Kubal et al., 2009).

In this study, different resources and methods were applied to a Portuguese drainage basin in order to obtain an estimate of the flood-prone area by: (1) field work reconstitution of past events involving the collection of historical data and hydrogeomorphological analyses and (2) hydrological-hydraulic simulation of four sections of the same basin area for which accurate topographic data was available.

The aim of the study was to estimate the flood-prone areas in a small drainage basin using two different methodological approaches, to compare their cartographic outputs and to evaluate the reproducibility of these complementary methods.

2   Study area

The study area is located in Central Portugal (Fig. 1) and lies within the parallels 40°09′14″ N and 39°46′33″ N and the meridians 8°43′06″ W and 8°28′18″ W. It corresponds to the Arunca River drainage basin, which is part of the Mondego River drainage basin. The main tributaries of the Arunca River, in terms of extent and constancy of flow, are the Anços River and the Valmar Stream on the right-hand bank and the Cabrunca River on the left-hand bank.

In geological terms, the Arunca drainage basin area includes sedimentary rocks – detritic rocks mainly from the Tertiary and limestone from the Jurassic. In the northern and western areas the outcropping rocks are predominantly detritic, whilst in the eastern area and part of the southern area of the basin limestone predominates. The altitudes in the basin range from 553 m in the eastern area (the geodesic vertex of Sicó) to almost three metres at the confluence with the Mondego River (the Arunca River mouth). The basin has a mean slope of about 11 % with a maximum value of 125 % in the area of the Sicó Calcareous Massif in the eastern area of the basin. From a hydrogeomorphological point of view the basin reveals contrasts: (a) the upstream valley presents moderate hills and a stream incision, (b) in the intermediate section, which is the most populated and urbanised area, the valley widens, has asymmetrical banks and the main stream begins to drain to the north and (c) in the lower course, still framed by asymmetrical banks, the valley is characterised by
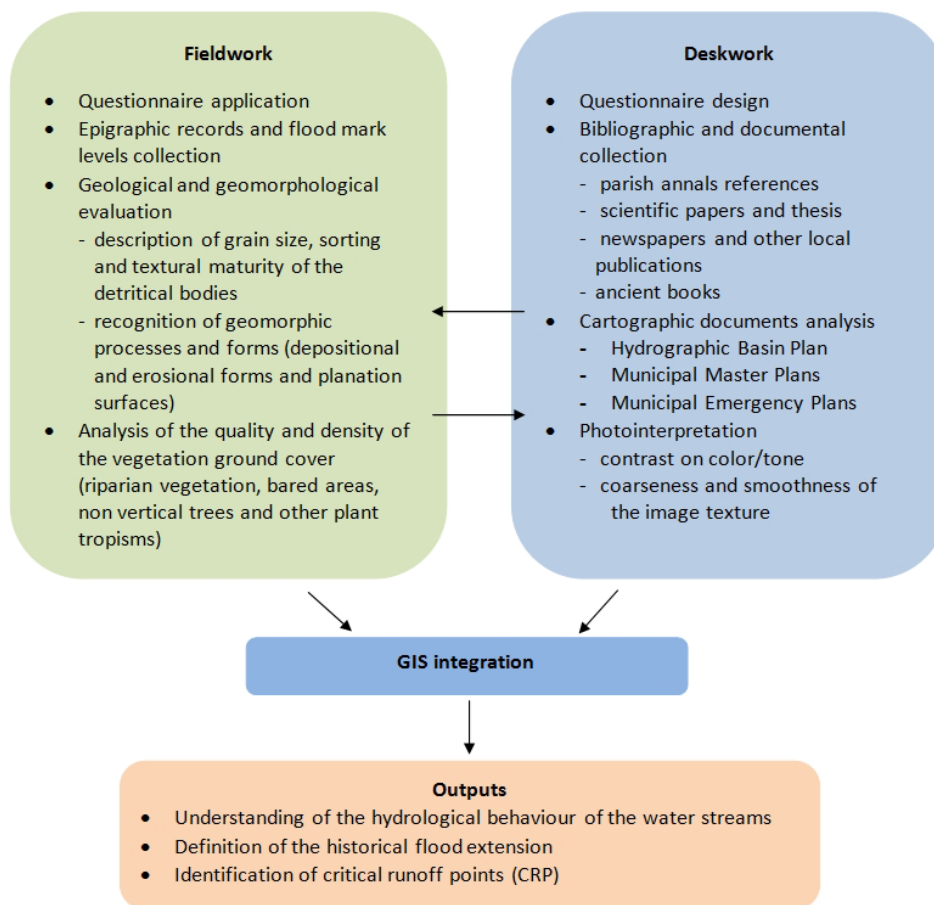
Fig. 3. Methodological approach for historical and hydrogeomorphological reconstitution.

a wide, flat plain extending to the confluence further downstream (Santos, 2009).

The area has a Mediterranean climate with hot summers and mild winters and a high orographic influence on rainfall (oceanic influences are revealed by rainfall, mainly in winter). The average monthly temperature ranges from 9 °C in January to 21 °C in August and the average annual rainfall is 964.6 mm (data from the series 1978/1979–2005/2006). The average monthly rainfall shows the contrast between the eastern area of the basin, with over 1200 mm yr^{-1}, and the western area, which has less than 900 mm yr^{-1}, mainly between October and January. Almost 20 % of the rainfall occurs in spring.

The main soil occupations (Fig. 2) are agricultural, with farmland and forest land occupying 42.9 % and 33.9 % of the total basin area respectively. The areas with a lower infiltration capacity correspond to only 2.5 % of the basin area and include urban, industrial/commercial and infrastructure areas. Wet zones, including areas used for growing rice, occupy a very similar area (2.1 %).

3 Methodology

Two different methodological approaches were used to estimate the inundated area of the Arunca River basin, which is frequently affected by floods.

The methodology was designed to deal with gaps in the primary data source and to obtain greater feasibility for the estimation of flood-prone areas.

3.1 Historical and hydrogeomorphological reconstitution

This analysis included historical and hydrogeomorphological methods which combined the collection of historical data relating to past events, a geological and geomorphological evaluation of the Arunca River basin following the case studies of Masson et al. (1996), Ballais et al. (2005), Coeur and Lang (2008) and Díez-Herrero et al. (2008), and a questionnaire administered to residents along the water streams in order to assess the flood hazard (e.g. Lastra et al., 2008). The basin area was subdivided into three sectors (A – downstream Soure, B – between Pombal and Soure and C – upstream

Pombal – see Fig. 1), an approach pointed out by Benito and Hudson (2010).

This method involved three main approaches: (i) field work, (ii) desk work and (iii) GIS integration, described below and summarised in Fig. 3. The first two approaches were performed simultaneously enabling the results to be integrated. This work took place from June 2007 to February 2008.

3.1.1 Fieldwork

A questionnaire was designed and administered to residents aged 18 or older living near the banks of the major streams of the basin and a final sample of 119 respondents was selected from the fieldwork. Along with this field inquiry, the authors gathered a total of 272 field notes. These records are intentional or purposeful ones with an exploratory objective. Nevertheless, considering an estimated population of 45 288 inhabitants, the confidence interval for this sample is 4.9 %, which means that the amount of field records collected is statistically strong.

The main groups of questions were designed to gather information on: (i) the limits of flood-prone areas, (ii) the maximum water column, (iii) land immersion time, iv) perceptions of the return period for major flooding, (v) evaluation of flow dynamics - from flash to progressive flood events, (vi) natural and anthropogenic triggering factors for floods and (vii) related damage and loss. A ratio of 1 questionnaire per 1.23 km of stream line was obtained.

All the questionnaires were geo-referenced for Geographic Information System integration using a GPS device (see examples in Fig. 4).

The fieldwork also involved the collection of nearly two hundred epigraphic records and flood high-water marks relating to past events over the entire Arunca River margin area and its tributaries (registered on bridges, houses, farm buildings, tree trunks and walls) cited by the local population. Most of these records refer to the flood of October 2006, the result of a 24 h rainfall of 104.8 mm, which is a value close to that estimated for the 100-yr return period (102.2 mm).

The fieldwork also enabled the analysis and interpretation of geomorphic forms and deposits associated with past floods. Sedimentary deposit outcrops (including a description of the grain size, sorting and textural maturity of the detrital bodies), identification of planation surfaces related to past floods events and incise channels eroded by torrential flows, enabled the recurring flood levels to be reconstituted. The sedimentary records were mapped and converted into digital data using a GIS support.

Analysis results of the quality and density of the vegetation ground cover ranged from riparian vegetation and bare areas associated with recent flash floods to leaning trees with identifiable impact marks. All this information was geo-referenced and converted into a digital format.
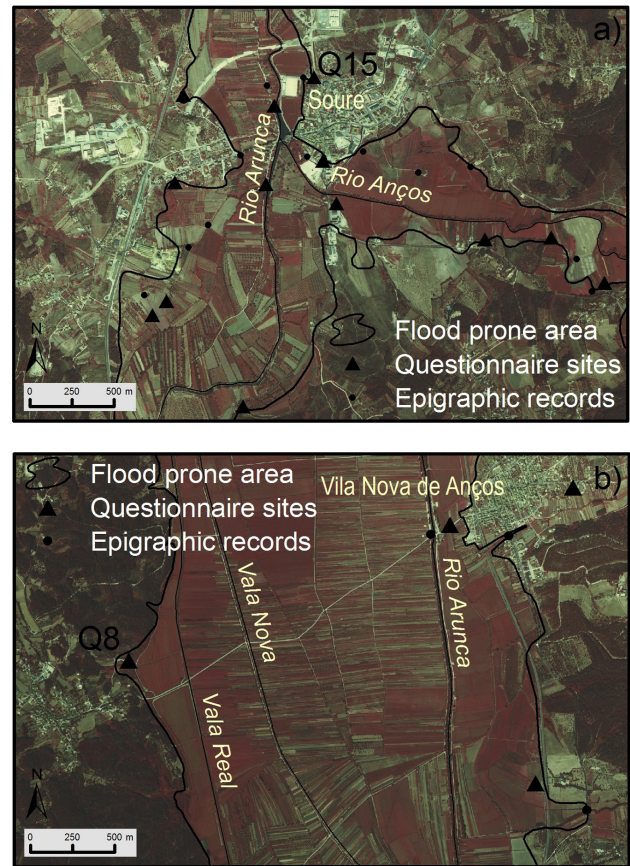

Fig. 4. Examples of field data collection. Water heights during last major flood event (2006) were 0.15 m in questionnaire site Q15 (**a**) and 1.5 m in Q8 (**b**).

3.1.2 Deskwork

Primary sources were collected including references in parish annals, scientific papers and theses, newspapers and other local publications and old books. Historical records of past floods in newspapers and other media are scarce. The information collected related mainly to damage and loss associated with human life and property. The oldest publication describing the impact of flooding dated from the 18th century (Costa, 1712).

Several cartographic documents from different sources were collected, such as maps of flood areas included in the Mondego River Hydrographical Basin Plan – MRHBP (INAG, 2000) and partial cartographic outputs from municipal master plans and emergency plans. All the existing cartographic representations were mainly constructed on a 1:25 000 scale, and, in material terms, recognised the alluvial deposits as the limit of the flood-prone area.

Consistent photointerpretation was produced with digital aerial false colour imagery on a 1:15 000 scale, using the Portuguese Geographical Institute resources. The digital
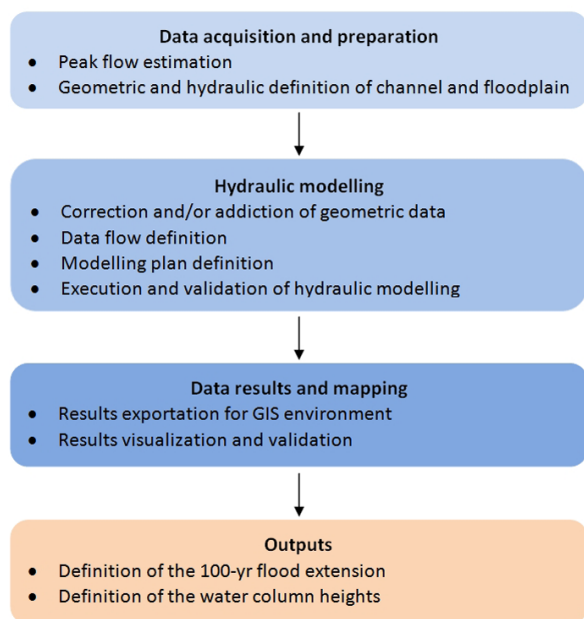
Fig. 5. Methodological approach for the hydrological-hydraulic method.

photography's sensitivity to green, red, and near-infrared radiation was particularly useful in delineating vegetation, wet soils and immature sedimentary deposits in the major stream valleys using colour/tone contrast, coarseness and smoothness of image texture.

As part of the deskwork, a Geographical Information System (GIS) was constructed, into which all the data collected from the fieldwork and deskwork was integrated, and then analysed using ESRI software ArcGIS and its 3-D and Spatial Analyst extensions. The GIS allowed for accurate and in-depth processing of the different sources of information, resulting in a definition of the maximum historical flood level.

The historical and hydrogeomorphological method resulted in two main outputs:

– the maximum historical flood extension, reported or collected as the wider inundated area, assumed to be the maximum fluvial flow for past events.

– a definition of critical runoff points (CRPs), consisting of locations where fluvial constraints, with or without associated damage, have been reported by the local population.

3.2 The hydrological-hydraulic method

The hydrological-hydraulic method was applied to four stream sections distributed along the Arunca River in order to map the 100-yr return period flood (see Fig. 6).

The hydrological-hydraulic method applied followed three main steps, as summarized in Fig. 5 and described in the following sections: (1) geometrical and flow data acquisition and preparation; (2) hydraulic modelling; (3) data results and mapping.

3.2.1 Data acquisition and preparation

Peak flow estimation

The Soil Conservation Service (SCS) method (see formulas in Table 1) was applied to estimate the 100-yr return period peak flow.

Rainfall intensity in mm h^{-1} (I) was obtained using the formula $I = aD^b$, in which D is the rainfall duration (min), assumed to be equal to the concentration time in each fluvial section, and a and b correspond to the parameter values for the Intensity-Duration-Frequency (IDF) curve, calculated and presented in the Mondego River Hydrographical Basin Plan (INAG, 2000): $a = 654.37$ and $b = -0.681$. The latter parameters result from the adjustment by the least-square method between rainfall intensity and duration associated with the 100-yr return period for durations of up to 24 h, as described in Brandão (1995). These procedures are referent to the nearest gauge station located in the city of Pombal using values from a 31 yr series. The adopted concentration time corresponds to the arithmetical mean for the values obtained using the Temez (1978), Chow (1964) and Soil Conservation Service (SCS, 1973) formulae (see formulas in Table 2). In Table 3 some intermediate parameter and final peak flow results are presented.

Geometric and hydraulic definition of channel and floodplain

Digital Terrain Models (DTM) for each section were obtained from maps on a scale of 1:2000 (2-m equidistant contours) and 1:10 000 (5-m equidistant contours). In addition to the hypsometric data obtained from the contours, these mapping sources also included hypsometric data from stream lines, roads and earthwork crests. Local data from aerial photographs, transversal sections, bridge profiles and field survey measurements were used to produce a more accurate morphological representation, involving better location and delineation of river embankments, bridges (including piers and decks) and railway levees.

After the DTM preparation in Triangulated Irregular Network (TIN) format, the ArcGIS extension HEC-GeoRAS version 4.2.92 (HEC, 2005) was used to extract the geometric and hydraulic elements required for subsequent hydraulic modelling (e.g. stream centerline, bank lines, cross sections, hydraulic structures and land use).

For each of the HEC-GeoRAS layers created, it was necessary to associate an attribute table containing information about its positioning along the cross-section. Finally, the geodatabase was exported in Extensible Markup Language (XML) format and, subsequently, in Spatial Data File (SDF) format so that it was readable in an HEC-RAS environment.

Table 1. Formulas for peak flow estimation using SCS method (from SCS, 1973).

Peak discharge (Q_p) in $m^3 s^{-1}$	$Q_p = \frac{RA}{3.6T_c}$	R - depth of runoff (mm)
		A – drainage area (km^2)
		T_c – concentration time (minutes)
Depth of runoff (R) in mm	$R = \frac{(p-I_a)^2}{(p-I_a)+S}$ if $p > I_a$	p – depth of 24-hr precipitation (mm)
		I_a – initial abstraction (mm); ($I_a = 0.2S$)
		S – maximum storage (mm)
Maximum storage (S) in mm	$S = \frac{25\,400}{CN} - 254$	CN – Runoff Curve Number corresponding to wet soil condition (AMC III) obtained in GRID format from SNIRH (2007)
Depth of 24-hr precipitation (p) in mm	$p = D_p\left(\frac{I_p}{60}\right)$	D_p – rainfall duration in minutes
		I_p – rainfall intensity in $mm\,h^{-1}$
Rainfall intensity (I_p) in $mm\,h^{-1}$	$I_p = a(T_c)^b,$	a and b – parameters from the Intensity-Duration-Frequency (IDF) curves

Table 2. Formulas for concentration time estimation (from Temez, 1978; Chow, 1964; SCS, 1973).

Method	Formula	
Temez (T_cT) in hours	$T_cT = 0.3\left(\frac{L}{J^{0.25}}\right)^{0.76}$	
Ven Te Chow (T_cV) in minutes	$T_cV = 25.2\left(\frac{L}{\sqrt{J}}\right)^{0.64}$	
Soil Conservation Service (T_cSCS) in hours	Maximum storage (S) in mm	$S = \frac{25\,400}{CN} - 254$
	Lag time (T_l) in hours	$T_l = L^{0.8}\left[\frac{(0.03937\,S+1)^{0.7}}{734.43(D_{med})^{0.5}}\right]$
	$T_c\,SCS = 1.67T_l$	

Where: L is the main stream length in km; J is the main stream average slope in $m\,m^{-1}$ for Temez formula and in % for Ven Te Chow formula; D_{med} is the basin average slope in %; CN is the Runoff Curve Number.

Table 3. Parameters and results regarding peak flow estimation.

	Section/Sub-basins	CN (AMC III)	Area (km^2)	Mean T_c (hours)	R (mm)	Q_p ($m^3 s^{-1}$)
1	Arunca River (upstream Vermoil)	86	64.55	4.16	34.85	135.88
	Small Arunca River tributary	89	0.78	0.66	15.62	4.58
2	Arunca River (upstream Pombal)	87	175.75	5.66	38.82	334.54
	Vale Stream (right tributary)	90	19.87	2.09	27.88	73.77
	Degolaço Stream (left tributary)	81	5.30	2.51	17.43	10.22
3	Arunca River (upstream Soure)	86	322.64	9.59	47.95	448.10
	Anços River (upstream Soure)	89	110.62	5.36	41.61	238.55
4	Arunca River (upstream Pt. Mocate)	88	469.80	10.41	54.09	765.92
	St. Isidro Stream (left tributary)	82	11.91	2.32	17.70	25.27
	S. Tomé Stream (1st right tributary)	82	5.57	2.45	18.36	13.65
	Sicó Stream (2nd right tributary)	82	6.19	1.96	15.91	13.93

Table 4. Geometric data in the four sections applications.

	Section	Reach length (km)	Reach slope (m m^{-1})	# cross sections	Average equidistance (m)
	1 – Ponte Vermoil	0.2	0.00594	30	7
	2 – Pombal	2.5	0.00338	393	6
3 – Soure	Arunca River (upstream confluence)	1.1	0.00129	106	10
	Arunca River (downstream confluence)	0.9	0.00175	194	5
	Anços River	1.2	0.00078	166	7
	4 – V. N. de Anços	3.5	0.00112	187	19

3.2.2 Hydraulic modelling

The 1-dimensional hydraulic modelling was performed with HEC-RAS software, version 3.1.3., designed by the Hydrologic Engineering Center of the United States Army Corps of Engineers (USACE), with RAS standing for River Analysis System (HEC, 2002a, b). The hydraulic modelling considered a steady and unidirectional flow. Computation between cross-sections was based on the solution of the 1-dimensional energy equation (HEC, 2002b).

The use of HEC-RAS tools can be subdivided into four phases: (a) correction and/or addition of geometric data for cross sections and hydraulic structures; (b) input of estimated peak flow data (for the main channel and its tributaries) and definition of boundary conditions (establishing the initial height of water), for which the normal depth slope method was selected using reach slope as a simplification of energy slope value as proposed in HEC (2002b). Observed flow data recorded at the Ponte Mocate gauge station was inserted in order to help calibrate the boundary flow conditions (see location in Fig. 8d and 9d); (c) general model plan definition – the geometry and flow data files previously prepared were assigned and a mixed flow regime was chosen; (d) execution and validation of hydraulic computations.

3.2.3 Data results and mapping

The computed 100-yr water surface profiles were exported to an HEC-GeoRAS- compatible format. Cross referencing this data with the DTM data in an ArcGIS environment enabled the flood extent and height mapping for the four fluvial sections modelled to be obtained.

3.2.4 Application areas

The 1-dimensional hydraulic model was applied to four sections of the Arunca River (Fig. 6): Sect. 1 (Ponte de Vermoil), Sect. 2 (Pombal), Sect. 3 (Soure) and Sect. 4 (Vila Nova de Anços). The sections were selected with the aim of covering the upper, middle and lower basin of the Arunca River,
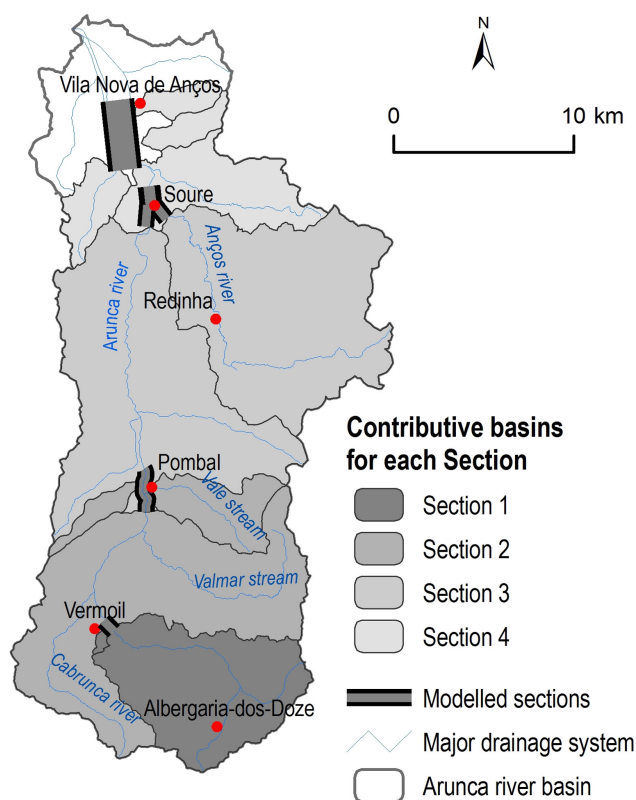
Fig. 6. Location of modelled sections and contributing drainage basins.

as well as urban and rural areas. However, the choice was strongly influenced by the availability of detailed cartography for the municipalities of Soure and Pombal (on a scale of 1:2000 for Sects. 1 and 2, and 1:10 000 for Sects. 3 and 4). Table 4 presents some geometric data for the modelled sections (application areas).

Section 1 corresponds to the smallest section modelled, located in the upper course of Arunca River, and is characterised by morphological changes associated with a bridge

Table 5. Flood-prone areas and number of critical runoff points (CRPs) in the Arunca basin.

Sector	Sector area (km^2)	Historic flood-prone area (km^2)	CRP
A – Downstream of Soure	110.75	17.24	32
B – Between Soure and Pombal	263.68	19.30	130
C – Upstream of Pombal	175.66	10.99	91
Total	550.09	47.53	253

Table 6. Water height for the flood-prone areas in the modelled sections

Height (m)		Area (%)					Total Area (ha)
		< 1 m	1–2 m	2–3 m	3–4 m	> 4 m	
	1	79.81	13.14	5.11	1.70	0.24	4.1
	2	66.51	26.48	1.81	0.95	4.25	102.8
Section	3	9.54	17.45	33.58	34.10	5.33	193.4
	4	9.37	19.30	26.83	31.32	13.19	706.7

and a road landfill construction. In Sects. 2 and 3, the fluvial stream modelled corresponds mainly to the urban areas of Pombal and Soure, respectively. These two sections cover the areas with the highest anthropogenic changes in the channel, margins and floodplain. In Sect. 3, two main rivers (the Arunca and the Anços – an Arunca River tributary) converge in the urban area of Soure. Finally, Sect. 4 corresponds to the lower sector of the Arunca alluvial plain, where it can be seen that the Arunca River flows in the most elevated (eastern) part of the floodplain.

3.3 Comparison methodology

The application of the hydrological-hydraulic method enabled the historical-hydrogeomorphological mapping to be accredited with an approximate recurrence interval and possible flood extension differentiator factors to be identified.

The results of Sects. 2, 3 and 4 were divided into several 200-m long blocks (12, 13 and 18 blocks, respectively) in order to quantitatively analyse the flooded areas, whereas the area in Sect. 1 was smaller and allowed for direct comparison. The Pearson correlation coefficient between the flood-prone areas obtained from both methods (in Sects. 2, 3 and 4) was used to evaluate the spatial adjustment of the cartographic outputs.

4 Results and discussion

4.1 Results of historical and hydrogeomorphological methods

These methods enabled the representation of the historical flood-prone area based on past evidences, and the identification of a total of 253 critical runoff points (CRPs).

Most of the flood problems were related to flash flood events (97 % of the total questionnaires); in the urban areas most of the reported floods were the result of overbank flow, underdimensioned pluvial sewer networks and unchannelled superficial runoff over impervious surfaces. The flood-prone areas associated with high flow were mainly restricted to the alluvial plain (north of Soure), with a sea tide influence on flood episodes reported in areas near the Arunca River mouth. According to the questionnaires, the water column reported was extremely variable – higher values (> three meters) were reported in the alluvial plain near the river bed. The most frequently reported average immersion time was between one and six hours, with the most prolonged floods (> two days) reported almost exclusively in Sector A.

The maximum historical flood extension and mapping of critical runoff points for the three sectors are presented in Fig. 7. It can be seen that in the entire Arunca River basin the historical flood represents a flood-prone area of 47.53 km^2, corresponding to nearly 8.6 % of the total basin area (Table 5) and a total of 253 CRPs were identified.

Most of the CRPs were recorded in Sector B (between Pombal and Soure), due to the urban areas of Soure and Pombal. In Pombal there is a runoff problem associated with the sewage and rainfall drainage system and the underground
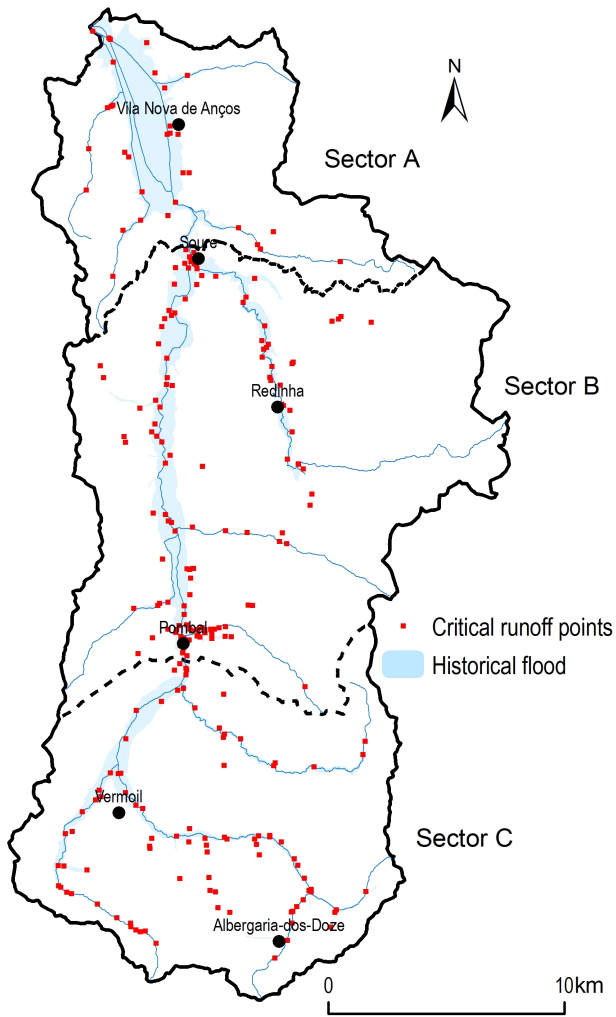
Fig. 7. Flood-prone areas and critical runoff points (CRPs).

drainage (with low flow section) of some water streams that cross the urban area. Some CRPs are related to an abrupt break in the longitudinal water stream profile. In Sector A (downstream of Soure), the CRPs are mostly associated with bridges and, in some cases, weirs.

4.2 Hydrological-hydraulic method results

The 100-yr flood maps resulting from 1-D modelling in HEC-RAS are presented in Fig. 8 for the four sections under consideration. The water height values for the flood-prone areas in each section are shown in Table 6.

In Sect. 1 most of the flooded area (79.81 %) presents a water height of less than one metre (Table 6); the areas with greater heights (>three metres) correspond to the Arunca channel bed. The bridge crossing the Arunca River in this section is submerged by an 11 cm water column over the bridge deck, and the road that crosses the floodplain on both
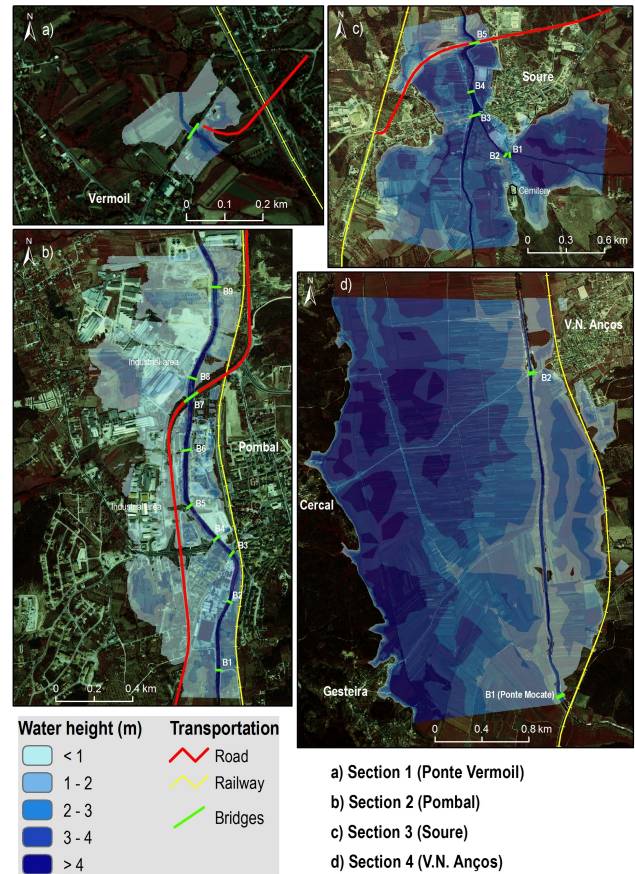

Fig. 8. Flood-prone areas and water height in the modelled sections.

sides of the bridge represents a clear obstacle to the flow, as can be seen in Fig. 8a.

In Sect. 2, the highest water column is around 5.5 m (see Fig. 8b), although the height of the flooded area is mainly less than one metre (Table 6). On the western side, the flood-prone area is more extensive, due to the larger dimensions of the left-hand bank of the Arunca River. On the eastern side of the area, the railway acts as a longitudinal embankment and prevents the flooding of some urbanised areas. In the central part of the modelled section, the existence of embankments prevents some areas from becoming flooded. Four of the nine existing bridges may be submerged (with 0.60 m to 1.60 m water columns over the bridge deck).

In Sect. 3 (Fig. 8c and Table 6), almost all the alluvial plain is flooded, with part of the historical urban area of Soure being exposed. It can be seen that most of the flooded area has a water column of over two metres, with some areas showing water heights of over six meters. The model indicates that three of the five existing bridges may be submerged (with 1.01 m to 3.10 m water columns over the bridge deck).The model also shows that a bridge (B5) obstructs the flow, imposing contrasting water column heights upstream and downstream of its location.
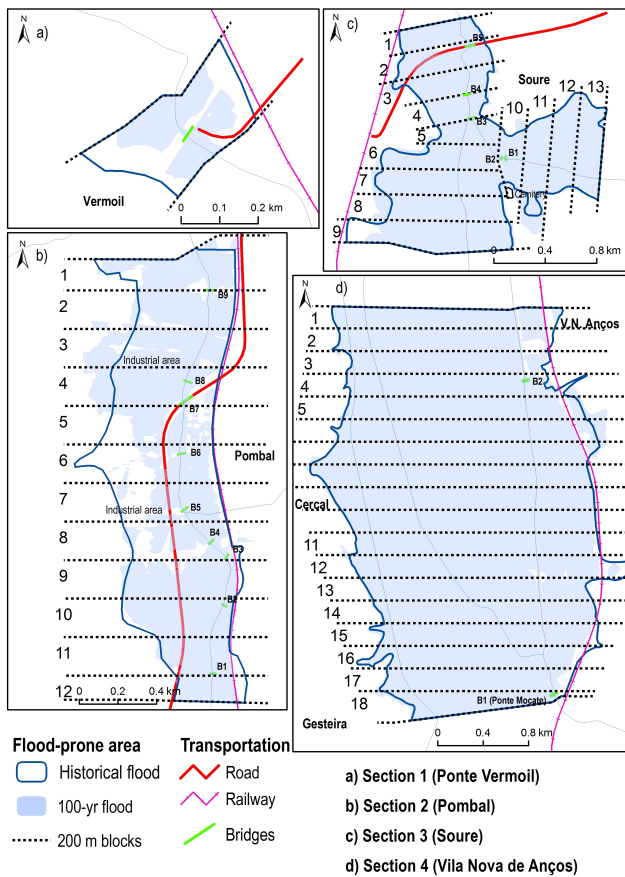
Fig. 9. Flooded areas in the modelled sections defined by both methods.

In Sect. 4, most of the flooded area involves water column heights of between three and four metres (Fig. 8d), corresponding to areas occupied by rice fields or permanently irrigated crops. The modelled results show that some roads crossing the alluvial plain will be submerged by a water column over three metres high and that the railway embankment acts as a restraining structure for flood expansion to the east. The asymmetric distribution of the water column heights can be verified, with areas of major water column height being located on the western side of the river bank, on the left-hand bank, and the lower heights contiguous to the Arunca River channel. This asymmetry is a consequence of the anthropogenic channelization of the Arunca River (previously flowing along the eastern side of the floodplain), which also determines the surge of inundated fields without any overbank flow for the Arunca River. In this section, one bridge (B2) may be submerged, with a 0.36 m water column above the bridge deck.

4.3 Comparison of results and discussion

The comparison of the results obtained by both methods is presented in Fig. 9 and Table 7 for each of the four sections

defined. Figure 10 presents the scatter plot of the flooded areas obtained by both methods for the various blocks defined in Sects. 2, 3 and 4, and the corresponding Pearson correlation coefficients (R).

In Sect. 1 (Fig. 9a), the flooded areas obtained by the two methods are very distinctive. The hydrological-hydraulic method gives a total flooded area that is almost 47 % lower than the flooded area resulting from historical and hydrogeomorphological reconstitution. This is explained by the successive removal of weirs which restrict flow and the enlargement and excavation of the river channel over the last three decades. The results demonstrate that there is a close cause-effect response between the flood-prone area and river channel interventions in the upper sector of the Arunca River basin.

In Sect. 2 (Fig. 9b), the flooded area obtained from the historical and hydrogeomorphological reconstitution (the maximum historical flood) is nearly 20 % greater than the area obtained by hydrological-hydraulic modelling (the 100-yr flood), presenting values of 122.36 ha and 102.79 ha, respectively (Table 7). In Fig. 10–Sect. 2, it can be seen that the correlation between the flooded areas of the various blocks defined in this section is very weak (0.455). This is due to the diverging values of the flood-prone areas obtained in blocks 5 to 8, as the exclusion of these blocks reflects a correlation of 0.927 (see the dashed line in Fig. 10). It is explained by significant morphological changes in these blocks (enlargement and excavation of the river channel and embankments in the industrial area). The obstruction created by the railway in the eastern part of the floodplain is very evident in Fig. 9b.

In Sect. 3 (Fig. 9c), the flooded areas defined by the two methods are more similar than in the previous sections, totalling 183.49 ha for the historical maximum flood and 193.43 ha for the 100-yr flood. The figures for the flood-prone areas obtained by both methods are very similar in almost all the blocks, resulting in a correlation value of 0.959 (Fig. 10 – Sect. 3).

In Sect. 4 (Fig. 9d), the flood-prone areas obtained by both methods are even more similar, with the flooded area corresponding to the 100-yr flood in this section, being only 1 % higher than the corresponding total maximum historic flood: the correlation coefficient is 0.978 (Fig. 10 – Sect. 4). The greatest similarity between flood limits can be observed in the left-hand sector of the floodplain and may be explained by the fact that this margin has fewer tributaries and there is a clearer transition between the floodplain and the hillside.

The results show that the data obtained from the population survey, the reconstructions of paleo-hydrogeomorphological characteristics and the systematisation of epigraphic records have a good match for the flood-prone area obtained by hydraulic modelling for an estimated return period of 100 yr, during which the floodplain, in general, preserved its natural topography. This was to be expected due to the occurrence of recent flood episodes, well

Table 7. Values for the flooded areas (ha) in Sects. 1, 2, 3 and 4 obtained using the historical and hydrogeomorphological method (HHG) and the hydrologic-hydraulic method (HH) – total and for each 200 m block defined.

Section		1		2		3		4	
		HHG	HH	HHG	HH	HHG	HH	HHG	HH
	Total	7.74	4.10	122.36	102.79	183.49	193.43	714.25	706.66
Block	1			11.28	10.11	11.09	11.58	35.81	33.90
	2			9.95	9.91	14.19	13.79	37.61	34.73
	3			10.47	12.67	12.60	13.73	34.75	33.74
	4			10.78	11.31	8.70	8.87	36.69	36.59
	5			10.91	6.69	8.69	9.06	41.35	42.15
	6			12.52	5.88	15.67	17.03	45.04	46.33
	7			10.89	6.56	19.10	20.48	46.95	47.60
	8			10.83	7.12	17.78	20.23	47.93	48.54
	9			11.90	11.21	27.11	24.42	45.82	46.64
	10			10.51	10.26	7.62	9.16	43.61	43.65
	11			7.46	7.11	13.07	16.63	42.80	42.41
	12			4.85	3.96	13.82	14.19	46.88	43.79
	13					14.05	14.27	39.41	39.59
	14							38.16	38.47
	15							38.44	37.45
	16							36.24	34.51
	17							32.73	31.42
	18							24.03	25.15

recognized in the local context, and related to precipitation events with a return period of more than 100 yr.

The four sections tested showed that the greater the width of the valley and number of control blocks, the better the match for the results obtained by both methods. In fact, Sect. 1 produced the worst results since it contained only two cross sections and a narrower alluvial bottom, while Sect. 4 with 19 blocks and the greatest width in the valley, produced a better match between the methods (see Figs. 9 and 10).

The results show that the response to the delineation of the flood-prone areas using the two methods is favourable in cases where the floodplains are bounded by embankments on the side of the main channel, associated with the (rail or road) transport network. In cases where the presence of bridges and embankments creates bottlenecks in the normal flow, a good match is obtained when the alluvial plain is wider.

Both methods show similar results when there is a confluence of two rivers (Sect. 3), showing that the hydraulic modelling results are consistent with historical and paleo-hydrogeomorphological reconstruction data.

The hydrologic-hydraulic method of defining flooded areas is more accurate in areas featuring topographic changes caused by human intervention and also in areas where the modelling database contains more details (e.g. geometry, roughness and flow). In contrast, the historical-hydrogeomorphological method produces better results in wide areas of the valley, expressing extreme flow conditions. It can also be seen that this method can be generalised more

easily for the whole basin, even though the database area is less reliable. In general, therefore, the study demonstrates that the historical-hydrogeomorphological method can easily be applied to the entire basin area, whilst the need for peak-flow, channel geometry and roughness data restricts application of the hydrological-hydraulic method. The importance of method complementarities should also be emphasised, especially in areas which lack data, in terms of the generalised application of the 1-D or 2-D hydrological-hydraulic approach.

5 Conclusions

With the historical-hydrogeomorphological method, the specific results for the area studied show a very significant flood-prone area in the Arunca River basin area, corresponding to almost 9 % of the total basin area and affecting the main urban areas located near water streams. The sections modelled using the hydrological-hydraulic method confirm the importance of the estimated inundated areas, and also clarify the significant impact on some urban areas with high water column values in the event of flooding (large submerged areas with depths of over 4 m were found, specifically in the urban areas of Pombal City and Soure Town). Both methods show the importance of the flood-prone areas regardless of the basin area that contributes with the flow, the morphology of the valley and the geometry and roughness of the channel.
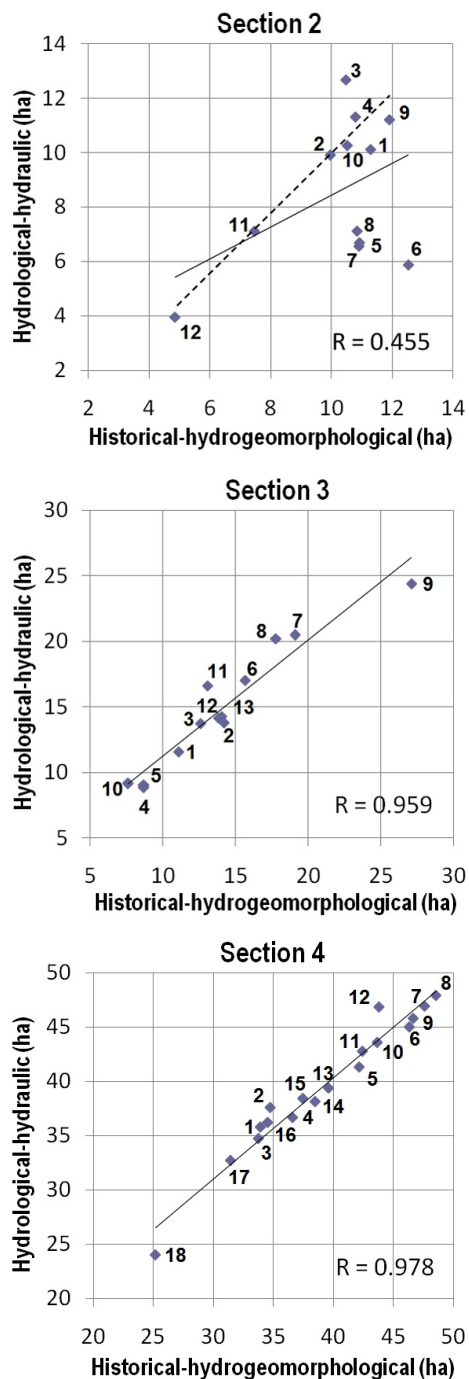
Fig. 10. Scatter plot of the flooded areas for Sects. 2, 3 and 4 obtained by both methods. *R* corresponds to the Pearson correlation coefficients (the dashed line in Sect. 2 represents the linear regression line excluding blocks 5 to 8).

As the historic flood-prone area reflects the hydraulic flow conditions prior to the anthropogenic changes to the Arunca channel, greater differences for the 100-yr flood-prone area appear when more changes are introduced due to anthropogenic influences. This leads to the conclusion that the

hydraulic-hydrologic method is sensitive to geometric inputs and is valid whilst these morphological conditions remain in place. On the other hand, the historical and hydrogeomorphological method tends to be more independent of time and does not reflect recent morphological changes in the floodplain. This has clear implications for the temporal validity of both types of flood-prone mapping, emphasising the importance of their combined use.

The reproducibility of this comparative approach is demonstrated by the importance of flood-prone area estimation, particularly in assuring the reliability of the historical-hydrogeomorphological method or in dealing with missing or inconsistent data used in hydrological-hydraulic modelling.

The complementarities of the methods made it possible to estimate the flood-prone area for the whole basin using historical-hydrogeomorphological reconstitution whilst hydrological-hydraulic modelling in areas with a more accurate database supports the 100-yr estimated return period. The application of both methods has generated new cartographic outputs: whereas identification of critical runoff points is obtained by historical-hydrogeomorphological reconstitution, the depth of the submerged area is obtained by hydrological-hydraulic modelling. These different cartographic outputs must be considered together when delineating the flood-prone areas, as complementary data collection allows for better management of the flooded areas by emphasising the data that controls the processes as well as the exposed elements. The complementary use of different methods to evaluate flood-prone areas needs to be used more extensively.

As final remarks, the use of these two methods to estimate the flood-prone areas highlighted their complementarities and the best performance for each method. In the specific studied area, certain innovative cartographic results made it possible to clearly upgrade the previous definition of the inundated areas. The study also indicated the tangibility of the results for other basin contexts by promoting the best approach for areas with insufficient or missing data, leading to improvements in flood management.

References

Apel, H., Aronica, G. T., Kreibich, H., and Thieken, A. H.: Flood risk analysis – how detailed do we need to be?, Nat. Hazards, 49, 79–98, 2009.

Ballais, J. L., Garry, G., and Masson, M.: Contribution de l'hydrogéomorphologie à l'évaluation du risque d'inondation:

le cas du Midi méditerranéen français, C. R. Geoscience, 337, 1120–1130, 2005.

Barriendos, M., Coeur, D., Lang, M., Llasat, M. C., Naulet, R., Lemaitre, F., and Barrera, A.: Stationarity analysis of historical flood series in France and Spain (14th20th centuries), Nat. Hazards Earth Syst. Sci., 3, 583–592, doi:10.5194/nhess-3-583-2003, 2003.

Barroca, B., Bernardara, P., Mouchel, J. M., and Hubert, G.: Indicators for identification of urban flooding vulnerability, Nat. Hazards Earth Syst. Sci., 6, 553–561, 2006, doi:10.5194/nhess-6-553-2006.

Benito, G., Díez-Herrero, A., and de Villalta, M. F.: Magnitude and frequency of flooding in the Tagus basin (Central Spain) over the last millennium, Clim. Change, 58, 171–192, 2003.

Benito, G. and Hudson, P. F.: Flood hazards: the context of fluvial geomorphology, in: Geomorphological hazards and disaster prevention, edited by: Alcántara-Ayala, I., Goudie, A., Cambridge University Press, Cambridge, 111–128, 2010.

Brandão, C.: Análise de precipitações intensas, MSc thesis, Universidade Técnica de Lisboa, Lisbon, 1995.

Casas, A., Benito, G., Thorndycraft, V. R., and Rico, M. : The topographic data source of digital terrain models as a key element in the accuracy of hydraulic flood modelling, Earth Surf. Proc. Land., 31, 444–456, 2006.

Chow, V. T.: Handbook of Applied Hydrology, McGraw-Hill, New York, 1964.

Coeur, D. and Lang, M.: Use of documentary sources on past flood events for flood risk management and land planning, C.R. Geoscience, 340, 644–650, 2008.

Costa, A.: Corografia Portugueza, e Descripçam Topográfica do Famoso Reyno de Portugal, 3, Oficina Real Deslandesiana, Lisboa, 1712.

de Moel, H., van Alphen, J., and Aerts, J. C. J. H.: Flood maps in Europe – methods, availability and use, Nat. Hazards Earth Syst. Sci., 9, 289–301, doi:10.5194/nhess-9-289-2009, 2009.

Díez-Herrero, A., Laín-Huerta, L., and Llorente-Isidro, M.: Mapas de peligrosidad por avenidas e inundaciones – Guía metodológica para su elaboración, Serie Riesgos Geológicos/Geotecnia, no. 1, Instituto Geológico Y Minero de España, 2008.

Fewtrell, T. J., Bates, P. D., Horritt, M., and Hunter, N. M.: Evaluating the effect of scale in flood inundation modelling in urban environments, Hydrol. Process., 22, 5107–5118, 2008.

Forte, F., Pennetta, L., and Strobl, R. O.: Historic records and GIS applications for flood risk analysis in the Salento peninsula (southern Italy), Nat. Hazards Earth Syst. Sci., 5, 833–844, doi:10.5194/nhess-5-833-2005, 2005.

Gül, G. O., Harmancıoğlu, N., and Gül, A.: A combined hydrologic and hydraulic modeling approach for testing efficiency of structural flood control measures, Nat. Hazards, 54, 245–260, 2010.

HEC: HEC-RAS, River Analysis System – User's Manual, Hydrologic Engineering Center – US Army Corps of Engineers, Davis, California, 2002a.

HEC: HEC-RAS, River Analysis System – Hydraulic Reference Manual, Hydrologic Engineering Center – US Army Corps of Engineers, Davis, California, 2002b.

HEC: HEC-GeoRAS, GIS Tools for Support of HEC-RAS using ArcGIS. User's Manual, Hydrologic Engineering Center – US Army Corps of Engineers, Davis, California, 2005.

IFRCRCS: World disasters report – Focus on early warning, early action, International Federation of Red Cross and Red Crescent Societies, 2009.

INAG: Plano de Bacia Hidrográfica do Rio Mondego, Water Institute, Lisbon, 2000.

Kubal, C., Haase, D., Meyer, V., and Scheuer, S.: Integrated urban flood risk assessment – adapting a multicriteria approach to a city, Nat. Hazards Earth Syst. Sci., 9, 1881–1895, doi:10.5194/nhess-9-1881-2009, 2009

Lastra, J., Fernández, E., Díez-Herrero, A., and Marquínez, J.: Flood hazard delineation combining geomorphological and hydrological methods: an example in the Northern Iberian Peninsula, Nat. Hazards, 45, 277–293, 2008.

Masson, M., Garry, G., and Ballais, J. L.: Cartographie des zones inondables. Approche hydro-géomorphologique, Paris La Défense, Les Editions Villes et Territoires, 1996.

Merz, B., Hall, J., Disse, M., and Schumann, A.: Fluvial flood risk management in a changing world, Nat. Hazards Earth Syst. Sci., 10, 509–527, doi:10.5194/nhess-10-509-2010, 2010.

Neal, J. C., Bates, P. D., Fewtrell, T. J., Hunter, N. M., Wilson, M. D., and Horritt, M. S.: Distributed whole city water level measurements from the Carlisle 2005 urban flood event and comparison with hydraulic model simulations, J. Hydrol., 368, 42–55, 2009.

Nirupama, N. and Simonovic, S. P.: Increase of flood risk due to urbanisation: A canadian example, Nat. Hazards, 40, 25–41, 2007.

Santos, P. P.: Cartografia de areas inundáveis a partir do método de reconstituição hidrogeomorfológica e do método hidrológico-hidráulico. Estudo comparativo na bacia hidrográfica do Rio Arunca, MSc thesis, 2009.

SCS: A Method for Estimating Volume and Rate of Runoff in Small Watersheds, Soil Conservation Service, U.S. Department of Agriculture, Washington, 1973.

SNIRH: Atlas da Água, Sistema Nacional de Informação de Recursos Hídricos, Water Institute, Lisbon, 2007.

Spaliviero, M.: Historic fluvial development of the Alpine-foreland Tagliamento River, Italy, and consequences for floodplain management, Geomorphology, 52, 317–333, 2003.

Sudhaus, D., Seidel, J., Bürger, K., Dostal, P., Imbery, F., Mayer, H., Glaser, R., and Konold, W.: Discharges of past flood events based on historical river profiles, Hydrol. Earth Syst. Sci., 12, 1201–1209, doi:10.5194/hess-12-1201-2008, 2008.

Temez, J. R.: Calculo Hidrometeorologico de Caudales Maximos en Pequeñas Cuencas Naturales, Ministerio de Obras Publicas y Urbanismo, Direccion General de Carreteras, 12, Madrid, 1978.

UNISDR: Global Assessment Report on Disaster Risk Reduction, United Nations, Geneva, Switzerland, 2009.

USGS: Facing Tomorrow's Challenges – U.S. Geological Survey Sciences in the Decade 2007–2017, Circular 1309, US Department of the Interior and US Geological Survey, Reston, Virginia, 2007.

Vijay, R., Sargoankar, A., and Gupta, A.: Hydrodynamic simulation of River Yamuna for riverbed assessment: a case study of Delhi region, Environ. Monit. Assess., 130, 381–387, 2007.